A Novel Space Vector Modulation Technique For Three Level NPC Converters Within Aircraft Starter Generator Systems

Chen Li[1], Giovanni Lo Calzo[2], Serhiy Bozhko[1], Chris Gerada[1], Patrick Wheeler[1], Tao Yang[1]

[1]*Power Electronics, Machines, Control(PEMC) group, University of Nottingham, NG7 2RD, Nottingham, UK*
[2]*Dyson Ltd, SN16 0RP, Malmesbury, UK*
<Chen.Li@nottingham.ac.uk, Tao.Yang@nottingham.ac.uk>

Keywords: Electric Starter Generator, Surface Mount PMSM, Three Level Neutral Point Clamped Inverter, Neutral Point Balancing.

Abstract

The neutral point voltage balancing issue for three level Neutral point clamped (NPC) converter has been extensively investigated recently. Different solutions to balance the neutral point have been proposed. However the proposed solutions so far either requires extra devices thus increasing the overall system size and weight or not desirable under low power factor, low pulse ratio and high modulation index conditions. This paper introduces a novel space vector modulation technique for an innovative aircraft starter generator system. The proposed method is capable of maintaining neutral point (NP) voltage balanced and ripple minimized at full power factor range, high modulation indices and low pulse ratio. The paper also provides detailed analysis into the sources of neutral point voltage imbalances and ripples. An aircraft electrical starter/generator system with a three-level NPC converter is studied in this paper. The simulation results in the Matlab/PLECS environment have demonstrated the effectiveness of the proposed technique.

1 Introduction

The newly emerged More Electric Aircraft (MEA) notion has triggered various movements to replace mechanical, pneumatic and hydraulic systems by their electrical counter parts, and existing electrical systems are being reformed into more efficient, compact systems [1]. However this introduces a dramatic increase of the demands for electrical power with extra burden laid on the electric power generation units.

The electrical starter generator technology represents the core of the MEA [2] as it leads to reduction of fuel
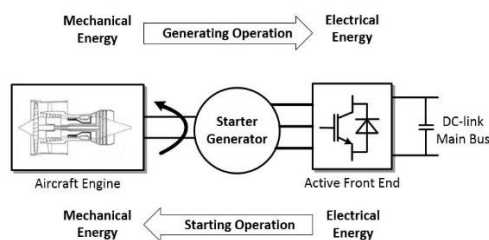

Fig1. Diagram of the target starter generator system

consumption, gas emission as well as overall system weight in comparison to previous generation systems. The current starter generator solution involves a three-stage wound field synchronous machine [3]. Despite being inherently safe for aircraft operation, the implementation of the starter function would require extra windings along with commutation devices, which puts extra layer of complexity on the readily sophisticated system.
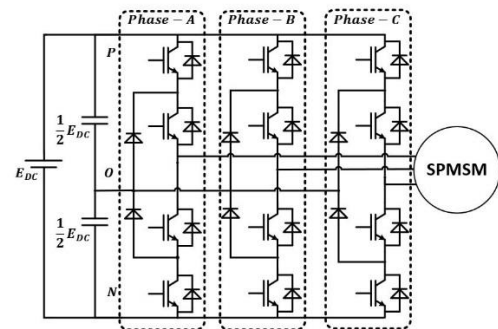

Fig2. Circuit diagram of a classic 3 level NPC converter

With the advancements of electric machine design and power electronics, a novel electric starter generator (ESG) system has been proposed [4] which could significantly improve the power density, efficiency and overall performance of the system. Depicted by Fig1, the system contains a Permanent Magnet Synchronous Machine (PMSM) connected to the engine shaft and a power electronic converter allowing bi-directional power flow. During starting operation, the system operates in motoring mode and active power flows from the converter into the PMSM. In generation mode, the active power being extracted from the PMSM to the converter and is used to power various loads in the aircraft.

Typically, the solution for the power converter is the two level inverter. However for improving the power quality and loss reduction, the three level neutral point clamped inverter topology is selected as the choice for the power converter [5]. In comparison to the conventional two level topology, 3-level NPC converter's advantage being the voltage stress on individual devices being halved, therefore the power rating could be potentially doubled with the exact same devices. The reduced voltage stress also leads to the reduction of switching losses, and the increased number of voltage levels reduces the distortions on the AC side phase currents.

However the use of the three level NPC converter leads to a common problem of the neutral point imbalance. The neutral

point imbalance of the NPC converter come in two categories. One category being the continuous DC imbalance between the upper and lower capacitor voltage, typically induced by imperfections within the converter or/and the load [6].

On the DC side, such imbalance would significantly increase the voltage stress placed on either capacitors and could cause capacitor failure or even explosion. On the AC side, continuous DC imbalance results in even order current harmonics, which could potentially aggravates the voltage imbalance, reduces the power quality and undermines machine operation.

The other category being the third harmonic ripple (AC imbalance) of the neutral point voltage, which is an inherent property of the NPC converter [7]. The amplitude of such ripple increases when the converter operates at low power factor and high modulation index, thus would require larger capacitors to absorb, otherwise this type of imbalance would also cause distortion of converter output voltage. Consequentially, larger-sized capacitors increases the volume and weight of the overall system and reduces power density.

For the continuous DC imbalance, the simplest approach is to modify phase voltage demands by injecting additional common-mode voltage [6]. Despite being simple, the effectiveness of such method is weakened at lower power factors. In case of no-load operation, when no active power being generated, the power flow between the converter and the PMSM becomes purely reactive, therefore average current into the neutral point of the DC-link is zero, and this method could potentially be instable. A number of more advanced and sophisticated methods based on common mode voltage injection were developed to alleviate the abovementioned issues [10], however their balancing ability are all tied to the amplitude of the load fundamental current. To untie the load fundamental current dependency, an alternative and intriguing method based on even order harmonic current injection was proposed [8]. It is established that the even order harmonic currents results in a non-zero average NP current [9], the method proposed in [9] injects an negative sequence third harmonic component into the voltage demands in synchronous reference frame, and second-order voltage demands can be obtained after the voltage demands being transformed from synchronous reference frame to phase voltage demands. This method covers the gap in low power factor operations and low fundamental load current operations at the expense of injecting distortions in the ac side.

For the 3rd harmonic AC imbalance, carrier based pulse width modulation methods typically adopts variable common mode voltage injection [10] whereas space vector modulation methods tend to manipulate the redundant small vectors [11]. These methods work effectively at low to medium modulation index. However, when the converter operates at high modulation index with low power factor such the NPC in the ESG system, the 3rd harmonic ripple becomes unavoidable. From the carrier based modulation point of view, common mode voltage injection methods would result in phase saturation (too much common mode injection) with very little influence on the ripple. For space vector based modulation, a virtual space vector modulation method was proposed [12], claiming capability of neutralizing the third harmonic ripple at all power factors. This method ties the duty cycles of small

vectors and the medium together, creating the virtual vector within each sector, which could achieve zero neutral point current within each switching period at DC balanced condition. However, such method results in larger switching loss, increased switching noise and EMI. In addition, the zero neutral point current within each switching period is based on the assumption that the phase currents stays constant throughout each switching period, which would not be inaccurate when the ratio between the switching frequency and the fundamental frequency is low (low pulse ratio), such as the aircraft starter generator applications. The solution for suppressing the third harmonic ripple is to install a pair of large capacitors whose size is dictated by zero power factor operation [7].

For both types of imbalance, there are also hardware solutions such as adding extra balancing circuit to charge or discharge the neutral point, having two capacitors supplied by separate DC sources and back to back operation. Since these solutions require extra circuitry, the size and the volume of the system would also increase, therefore they are not discussed within the context.

Despite the neutral point balancing issue is widely discussed in the past [7],[9],[13], the unique operating characteristics of starter-generator system such as high fundamental frequency, severe limitations on overall system size and volume, as well as limited impact on the AC side requires a specific solution for the problems.

This paper proposes an alternative space vector modulation method suitable for three level NPC converter used in aircraft starter generator applications. This method is capable of neutralizing the continuous DC imbalance and 3rd harmonic ripple of the neutral point voltage at high modulation index and at all power factors.

For the structure of the paper, Section II provides a brief description of the studied starter-generator control structure, Section III expands the causes of the type I and type II imbalances, Section IV presents the newly proposed space vector modulation technique and a comparison to the conventional virtual space vector based modulation scheme, Section V presents initial simulation results of the proposed modulation scheme.

2 ESG System Configuration and Control

Fig3. Control structure for the proposed S/G system

For the starter-generator machine [14], a 6-pole 36-slot surface mount PMSM is designed and classic vector control structure with synchronous reference frame current regulators is selected. When the speed of the machine is beyond the base speed, flux weakening operation is activated and negative d-axis current is injected based on the error between the reference voltage and the voltage limit set by the inverter. The q-axis current reference is set by the outer speed loop when the system operates in starter mode. During flight, the system operates in generating mode and the q-axis current reference is set by the DC-link current demands dictated by droop control [15]. In such circumstances, both q-axis and d-axis currents are negative, therefore the power factor is typically very low. In addition, the flux weakening operation requires almost full utilization of the DC-link voltage, therefore a high modulation index is expected.

As the machine operates at between 20000rpm and 32000rpm in generating mode, the fundamental frequency is between 1000Hz and 1600Hz, therefore the resultant pulse ratio is between 16 and 10, assuming a switching frequency of 16kHz is selected.
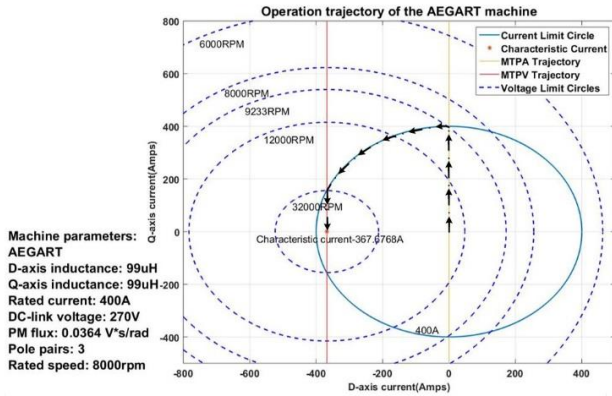
Fig4. Operating trajectory of the target system

In summary, the modulation scheme for the converter must maintain neutral point balance at constantly high modulation index, low power factor and low pulse ratio.

3 NPC SVM analysis

3.1 Principle of Operation

A total number of 27 states are available for a three level NPC converter. As illustrated in Fig5, the orange ones are large vectors with magnitudes of $\frac{2}{3}V_{pn}$, which connect all three phases to either positive or negative rail, therefore do not affect the neutral point potential. The purple ones are null vectors, where all three phases are connected to the same rail, and no current would be flowing, therefore the neutral point potential is not affected as well. The vectors in blue are medium vectors with the magnitude of $\frac{\sqrt{3}}{3}V_{pn}$, which connects three phases to the positive rail, the negative rail and the neutral point, vector PNO for example, connects phase C to the neutral point, therefore phase current i_c is supplied by the neutral point, affecting the neutral point potential. The green

vectors are small vectors with magnitudes of $V_{pn}/3$, as they come in pairs with opposite polarity of neutral point current, they could be used to mitigate the neutral point potential affected by the medium vectors, which are not controllable.

The conventional space-vector modulation synthesize the reference voltage vector in the stationary reference frame
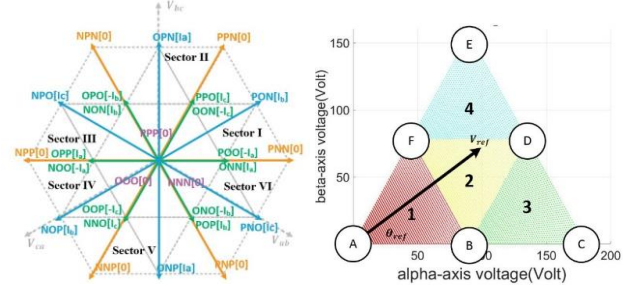
Fig5. Available switching states and neutral point currents (left)
Fig6. Synthesis of reference voltage in SVM (right)

based on the nearest three space vectors (N3V) as in Fig6, where the triangle represents one of the six sextants of the space vector hexagon in Fig5, and vector A represents the null vector, vector B & F represents the small vectors, vector D represents the medium vector and vector C & E represents the large vector. The duty cycle of each vector is calculated based on voltage-time-area balance between the selected voltage space vectors and the reference vector, for example, a reference vector falls inside the region3 in Fig6 can be calculated from (1) and (2):

$$V_{ref} = d_B V_B + d_C V_C + d_D V_D \qquad (1)$$
$$d_B + d_C + d_D = 1 \qquad (2)$$

3.2 Source of Neutral Point Imbalance

With the modulation technique described in Section 3.1, the neutral point is being charged or discharged when the medium vector and the small vectors are applied. The voltage difference between the upper and the lower capacitor induced within each switching period can be summarised as:

$$\Delta V_{NP} = \frac{1}{C} \int_0^{T_s} i_{NP} \, dt \qquad (3)$$

where C represents the DC-link capacitor capacitance.

For the medium vector V_D and the small vectors V_B and V_F, their neutral point current-time-area within each switching period are:

$$ITA_D = T_s \cdot d_D \cdot S_D(sector)$$
$$ITA_B = T_s \cdot d_B \cdot S_B(sector) \qquad (4)$$
$$ITA_F = T_s \cdot d_F \cdot S_F(sector)$$

where T_s represents a switching period, d_x represents corresponding duty cycle, S_D, S_B and S_F are neutral point

Sector	$S_D(sector)$	$S_B(sector)$	$S_F(sector)$
I	i_b	i_a	i_c
II	i_a	i_c	i_b
III	i_c	i_b	i_a
IV	i_b	i_a	i_c
V	i_a	i_c	i_b
VI	i_c	i_b	i_a

Table1. Definitions of current switching functions

3

current switching functions defined for the medium vector V_D and the small vectors V_B and V_F:

Only to consider the fundamental component of the AC side currents, the neutral point potential drift induced by the small vectors and the medium vector over a line cycle are mapped using (3), (4) and table1 shown in Fig7.
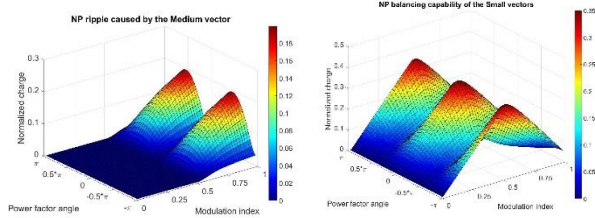

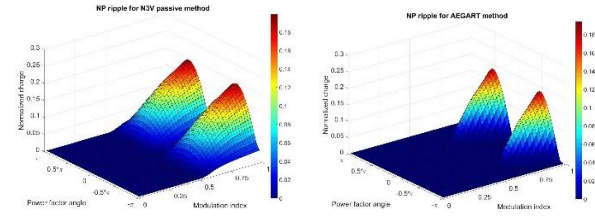Fig7. Neutral point potential drift from a) V_D b) V_B, V_F

Fig8. Neutral point ripple a) without b) with control

It can be seen that the medium vector places a large impact on the neutral point potential at high modulation index and low power factor, whereas the balancing ability defined by the current-time-area of the small vectors are stronger at moderate modulation index with higher power factor.

Conventional space vector modulation technique for NPC converter swap the polarity of the small vectors in alternate switching periods instead of manipulating them against the medium vector within each switching period [7]. This method effectively cancels the balancing ability of the small vector and leaves the disturbance from the medium vector untouched, therefore can serve as a benchmark for various neutral point balancing modulation approaches. The extent of the 3rd harmonic neutral point potential ripple with and without manipulation of small vectors are presented in Fig8, it can observed that the manipulation of the small vectors can reduce the extent of the neutral point ripple, however at very high modulation index and lower power factor, the extent of the ripple remains almost unchanged.

4 The proposed modulation scheme

4.1 Region and duty cycle computation

The proposed space vector modulation restricts the use of the medium vector at higher modulation index, therefore the sectors are divided as given in Fig9 & 10. In region 1, the reference vector is synthesized by the null vector and two small vectors, and the duty cycles for each vector are given in (5).

$$d_B = 2 \cdot M \cdot \sin(\frac{\pi}{3} - \theta_{ref})$$
$$d_F = 2 \cdot M \cdot \sin(\theta_{ref})$$
$$d_A = 1 - d_B - d_F$$
(5)

In the second region, the reference voltage vector is synthesized by the medium vector and the two small vectors. The duty cycles for each vector are given in (6).
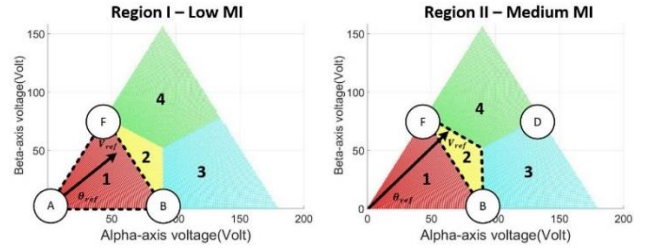
Fig9. Proposed SVM a) region 1 b) region 2

$$d_B = 1 - 2 \cdot M \cdot \sin(\theta_{ref})$$
$$d_F = 1 + 2 \cdot M \cdot \sin(\theta_{ref} - \frac{\pi}{3})$$
$$d_D = 2 \cdot M \cdot \sin\left(\theta_{ref} + \frac{\pi}{3}\right) - 1$$
(6)
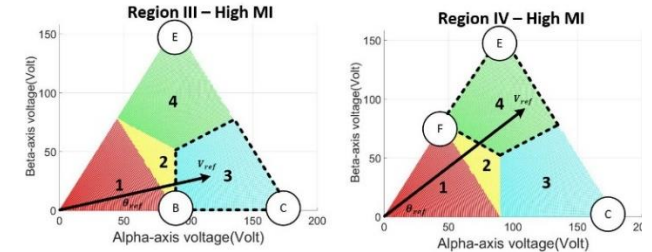
Fig10. Proposed SVM a) region 3 b) region 4

In the third and the forth region, the reference voltage vector is synthesized by two large vectors and the adjacent small vector. The duty cycles for each vector are given in (7) and (8).

$$d_B = 2 - 2 \cdot M \cdot \sin(\theta_{ref} + \frac{\pi}{3})$$
$$d_C = \sqrt{3} \cdot M \cdot \cos(\theta_{ref}) - 1$$
$$d_E = M \cdot \sin(\theta_{ref})$$
(7)

$$i_a = \hat{I}_s \cos(\omega t - \varphi) + \sum_{n=2}^{\infty} \hat{I}_n \cos(n\omega t - \varphi_n)$$

$$i_b = \hat{I}_s \cos(\omega t - \frac{2}{3}\pi - \varphi) + \sum_{n=2}^{\infty} \hat{I}_n \cos[n(\omega t - \frac{2}{3}\pi) - \varphi_n]$$

$$i_c = \hat{I}_s \cos(\omega t + \frac{2}{3}\pi - \varphi) + \sum_{n=2}^{\infty} \hat{I}_n \cos[n(\omega t + \frac{2}{3}\pi) - \varphi_n]$$
(4)

$$d_C = M \cdot \sin\left(\theta_{ref} - \frac{\pi}{3}\right)$$

$$d_E = \sqrt{3} \sin\left(\theta_{ref} + \frac{\pi}{6}\right) - 1 \qquad (8)$$

$$d_F = 2 - 2 \cdot M \cdot \sin\left(\theta_{ref} + \frac{\pi}{3}\right)$$
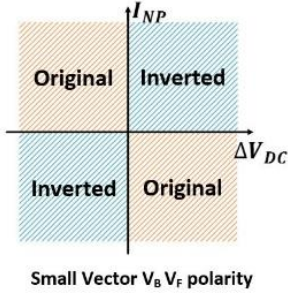
4.2 Small vector polarity manipulation

Fig11. Small vector polarity determination

Within each switching period, the arrangement of the switching pattern is organized in such a way that the use large vectors are placed at the sides whereas the small vector is kept at the centre, thus forming a half-wave symmetrical pattern. The critical part of the proposed space vector modulation technique resides in the approach to determine the polarity of the small vector at the presence of neutral point potential drift. Presented with Fig11, one approach is to determine the polarity of the small vector based on measured neutral point current and imbalance of DC-link capacitor voltages. The current flowing into the neutral point can be determined by the current switching functions for small vectors defined in Table1, whereas the imbalance of DC-link capacitor voltages is defined by (9).

$$\Delta V_{DC} = V_{c1} - V_{c2} \qquad (9)$$
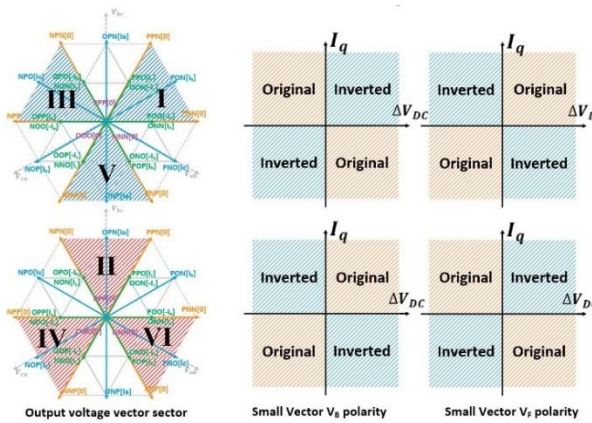
Fig12. Small vector polarity determination

Assuming the reference voltage falls inside the third region of the first sector, the upper capacitor voltage is larger than that of lower one, and the phase-a current is larger than zero, switching pattern would be: PNN-PPN-POO-PPN-PNN

Alternatively, the polarity can also be determined by the active power flowing within the system and the imbalance of DC-link capacitor voltages. Presented in Fig12, the polarity of the small vector depends on the sector of the reference voltage vector as well as the direction of the q-axis current. Assuming the voltage space vector falls inside the third region of the first sector, the system operates in generator mode with a negative q-axis current, and the upper capacitor voltage is larger than that of the lower one, the switching pattern would be: PNN-PPN-ONN-PPN-PNN.

The performance of the two presented methods are complementary, as the second method is more suitable when there is active power flowing between the machine side and the converter side, whereas the first method can deliver better performance when the system is operating in standby mode and the power flowing within the starter-generator system is predomiantly reactive, despite it might be prone to phase current zero crossing issues at certain power factors.

5 Simulation results

A simulation model for the SPMSM based starter generator system is built in the PLECS/Simulink environment. Simulation results for a typical starting/generating process are presented in Fig13 and Fig14. The system operates in starter mode initially, during which the machine acts at motor and active power flows from the NPC converter to the machine, accelerating the engine to the ignition speed. The flux weakening operation starts at approximately 0.45s when the machine back-emf exceeds the DC-link voltage.

Followed by the ignition of the engine, the S/G system maintains a self-sustaining speed of 20krpm and the system switches to generator mode. The droop control takes over the DC-link voltage regulation, generating q-axis current references to the inner current controller. A 15kw resistive load is applied to the system by connecting to the DC-link, resulting in a droop of the overall DC-link voltage and a step increase of negative q-axis current. It is worth noting that a large negative d-axis current is constantly required for flux weakening in generating mode, as the speed of the S/G system is constantly above the threshold value. This indicates the system constantly operates at low power factor with high modulation index, and pushes the NPC converter into operating at ripple-prone region (denoted in red in Fig8(b)).

Both N3V and the proposed modulation method are evaluated in simulation. Corresponding DC-link capacitor voltage variations, converter output line voltage and ac side phase current along with THD results are presented in Fig15 to Fig7 respectively.

It can be observed from the simulation results that the proposed modulation technique eliminates the DC imbalance and significantly reduces the AC imbalance of the neutral
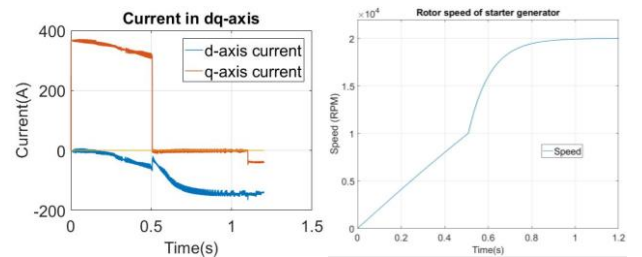

Fig13. S/G system dq-axis currents in typical starting/generating process
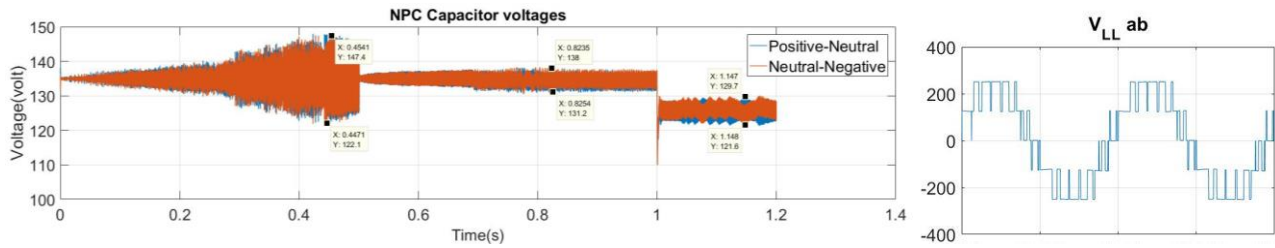Fig14. S/G system speed characteristics in simulation (right)

Fig15. Nearest three vector method a) Variation of capacitor voltages in starter/generator operation b) Line to line voltage
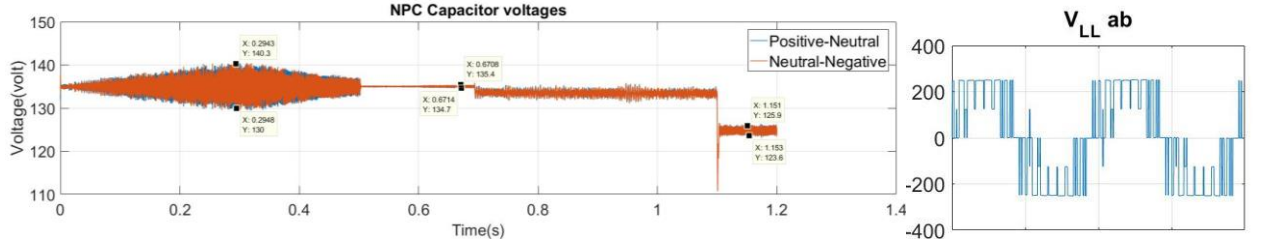

Fig16. The proposed method a) Variation of capacitor voltages in starter/generator operation b) Line to line voltage
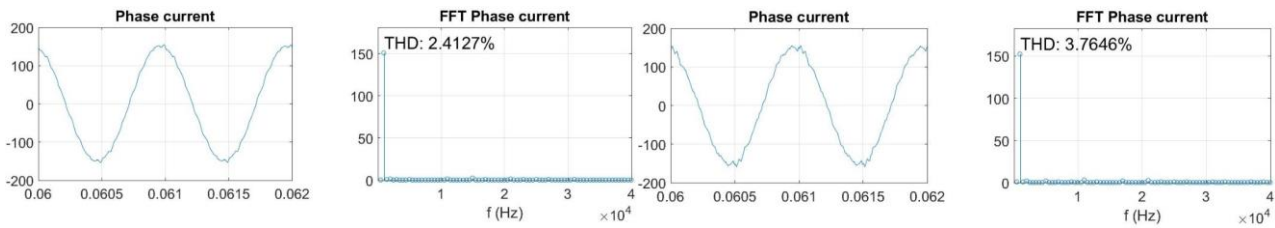

Fig17. Time and frequency domain results of phase currents for a) Nearest three vector method b) The proposed method

point potential at the expense of slightly compromising ac side output voltage. However, the harmonics induced in the ac side currents limited, evident by the presented current THD results.

6 Conclusion

A novel space vector modulation technique for three level NPC converter used in aircraft starter generator system is presented in the paper. The method is proven by simulation capable of maintaining the neutral point voltage balanced with reduced ripple without significantly impairing the AC side harmonic performance. Experimental validation of the proposed method is being carried out with a high speed aircraft starter generator platform.

Acknowledgements

References

[1] P. Wheeler and S. Bozhko, "The More Electric Aircraft: Technology and challenges.," *IEEE Electrif. Mag.*, Dec. 2014.

[2] S. Bozhko, M. Rashed, C. I. Hill, S. S. Yeoh, and T. Yang, "Flux Weakening Control of Electric Starter-Generator Based on PMM," *IEEE Trans. Transp. Electrif.*, pp. 1–1, 2017.

[3] F. Gao, *Decentralised Control and Stability Analysis of a Multi-Generator Based Electrical Power System for More Electric Aircraft*, no. August. 2016.

[4] S. Bozhko, S. S. Yeoh, F. Gao, and C. Hill, "Aircraft starter-generator system based on permanent-magnet machine fed by active front-end rectifier," in *IECON 2014 - 40th Annual Conference of the IEEE Industrial Electronics Society*, 2014, pp. 2958–2964.

[5] R. Teichmann and S. Bernet, "A comparison of three-level converters versus two-level converters for low-voltage drives, traction, and utility applications," *IEEE Trans. Ind. Appl.*, vol. 41, no. 3, pp. 855–865, 2005.

[6] C. Newton and M. Sumner, "Neutral point control for multi-level inverters: theory, design and operational limitations," in *IAS '97. Conference Thirty-Second IAS Annual Meeting*, vol. 2, pp. 1336–1343.

[7] N. Celanovic and D. Boroyevich, "A comprehensive study of neutral-point voltage balancing problem in three-level neutral-point-clamped voltage source PWM inverters," *IEEE Trans. Power Electron.*, vol. 15, no. 2, pp. 242–249, Mar. 2000.

[8] M. Marchesoni, P. Segarich, and E. Soressi, "A new control strategy for neutral-point-clamped active rectifiers," *IEEE Trans. Ind. Electron.*, vol. 52, no. 2, pp. 462–470, 2005.

[9] J. Pou, D. Boroyevich, and R. Pindado, "Effects of Imbalances and Nonlinear Loads on the Voltage Balance of a Neutral-Point-Clamped Inverter," *IEEE Trans. Power Electron.*, , Jan. 2005.

[10] C. Wang and Y. Li, "Analysis and calculation of zero-sequence voltage considering neutral-point potential balancing in 3LNPC converters," *IEEE Trans. Ind. Electron.*, vol. 57, no. 7, pp. 2262–2271, 2010.

[11] Y. Jiao, F. C. Lee, and S. Lu, "Space vector modulation for three-level NPC converter with neutral point voltage balance and switching loss reduction," *IEEE Trans. Power Electron* 2014.

[12] S. Busquets-Monge, J. Bordonau, D. Boroyevich, and S. Somavilla, "The nearest three virtual space vector PWM - a modulation for the comprehensive neutral-point balancing in the three-level NPC inverter," *IEEE Power Electron. Lett.*, vol. 2, no. 1, pp. 11–15, Mar. 2004.

[13] J. Shen, S. Schroder, B. Duro, and R. Roesner, "A Neutral-Point Balancing Controller for a Three-Level Inverter With Full Power-Factor Range and Low Distortion," *IEEE Trans. Ind. Appl.*, vol. 49, no. 1, pp. 138–148, Jan. 2013.

[14] S. S. Yeoh, T. Yang, L. Tarisciotti, C. I. Hill, S. Bozhko, and P. Zanchetta, "Permanent Magnet Machine based Starter-Generator System with MMPC," *IEEE Trans. Transp. Electrif.*, 2017.

[15] F. Gao, S. Bozhko, A. Costabeber, G. M. Asher, and P. W. Wheeler, "Control Design and Voltage Stability Analysis of a Droop-Controlled Electrical Power System for More Electric Aircraft," *IEEE Trans. Ind. Electron.*, pp. 1–1, 2017.